Received: 31 January 2020 | Revised: 22 March 2020 | Accepted: 23 March 2020

DOI: 10.1111/gcb.15107

PRIMARY RESEARCH ARTICLE

Global Change Biology WILEY

Contribution of unvegetated tidal flats to coastal carbon flux

Wei-Jen Lin[1] | Jihua Wu[2] | Hsing-Juh Lin[1]

[1]Department of Life Sciences and Innovation and Development Center of Sustainable Agriculture, National Chung Hsing University, Taichung, Taiwan

[2]Ministry of Education Key Laboratory for Biodiversity Science and Ecological Engineering, Coastal Ecosystems Research Station of the Yangtze River Estuary, Institute of Biodiversity Science, School of Life Sciences, Fudan University, Shanghai, China

Correspondence
Hsing-Juh Lin, Department of Life Sciences and Innovation and Development Center of Sustainable Agriculture, National Chung Hsing University, Taichung 40227, Taiwan.
Email: hjlin@dragon.nchu.edu.tw

Funding information
Kinmen National Park Headquarter; Mainland Affairs Council of Taiwan; National Natural Science Foundation of China, Grant/Award Number: 41871035 and U1405234; Ministry of Education (MOE) of Taiwan

Abstract

Unvegetated flats occupy a large area in the intertidal zone. However, compared to vegetated areas, the carbon sequestration of unvegetated tidal flats is rarely quantified, even though these areas are highly threatened by human development and climate change. We determined benthic maximum gross primary production (GPP_m), net primary production (NPP) and total respiration (TR) during emersion on seven tidal flats along a latitudinal gradient (from 22.48°N to 40.60°N) in winter and summer from 2012 to 2016 to assess the spatial and temporal variability of carbon dioxide flux. In winter, these processes decreased by 89%–104% towards higher latitudes. In summer, however, no clear trend was detected across the latitudinal gradient. Quadratic relationships between GPP_m, NPP and TR and sediment temperature can be described along the latitudinal gradient. These curves showed maximum values of GPP_m and NPP when the sediment temperatures reached 28.7 and 26.6°C respectively. TR increased almost linearly from 0 to 45°C. The maximum daily NPP across the latitudinal gradient averaged 0.24 ± 0.28 g C m^{-2} day^{-1}, which was only 10%–20% of the global average of NPP of vegetated coastal habitats. Multiplying with the global area of unvegetated tidal flats, our results suggest that the contribution of NPP on unvegetated tidal flats to the coastal carbon cycle is small (11.04 ± 13.32 Tg C/year). If the land cover of vegetated habitats is continuously degraded to unvegetated tidal flats, the carbon sequestration capacity in the intertidal zone is expected to reduce by at least 13.10 Tg C/year, equivalent to 1% of global carbon emissions from land-use change.

KEYWORDS

benthic metabolism, blue carbon, gross primary production, land-use change, latitudinal gradient, microphytobenthos, net primary production, respiration

1 | INTRODUCTION

The coastal intertidal zone between terrestrial and marine environments provides a variety of ecosystem services to humans, such as nutrient cycling, biodiversity and food production (Costanza et al., 1997). Vegetated coastal habitats, such as mangroves, seagrass beds and salt marshes, are recognized as blue carbon sinks (Nellemann et al., 2009) and play a significant role in the global carbon cycle (Chiu, Huang, & Lin, 2013; Huang, Lee, Chung, Hsiao, & Lin, 2015; Li et al., 2018). However, the large occupied but much less studied areas in this zone are unvegetated tidal flats, which are generally located at the fringes of vegetated habitats or coasts that are unsuitable for vegetation. The global extent and distribution of unvegetated tidal flats have not been comprehensively assessed. Recently, the global area of tidal flats was estimated to be 127,921 km^2, mainly distributed in Asia (44% of total; Murray et al., 2019). However, this estimate does not include areas at a latitude higher than 60°N. The estimated global area of unvegetated tidal flats was 2.32 times that of salt marshes, comparable to that of mangroves, and only 16% of that of seagrass beds (Davidson & Finlayson, 2019).

In the past few decades, tidal flats have been highly threatened by human development, such as land claims (Chen et al., 2016). Since 1984, unvegetated tidal flats have declined by the rate of 16.02%, which suggests a potential loss of more than 20,000 km^2 globally (Murray et al., 2019). Regionally, up to 65% of tidal flats in the Yellow Sea were lost from 1950 to 2000 (Murray, Clemens, Phinn, Possingham, & Fuller, 2014), and 31% of tidal flats in the Yangtze Estuary have been lost in the past three decades (Chen et al., 2016). Tidal flats are also vulnerable to accelerated sea-level rise (Galbraith et al., 2002; Kirwan & Megonigal, 2013). Recently, tidal flats in China and elsewhere are threatened by the invasion of *Spartina alterniflora* (Li et al., 2009), which may change the abundance and community of benthic invertebrates and ultimately affect the function as a feeding ground for shorebirds (Lin, Hsu, Liao, Chen, & Hsieh, 2015). Under the threat of human impacts and climate change, it is crucial to quantify the capacity and examine the regulating factors of carbon sequestration on tidal flats. Any change in the carbon sequestration on tidal flats might be significant to the global carbon budget due to the large area of such habitats on the global scale. However, tidal flats are neglected in current global carbon budget models, and the understanding of carbon sequestration of these areas would fill the critical gap.

When vascular plants are not the primary producers on tidal flats, benthic macro- and microalgae often inhabit the surface of sediment. Ephemeral macroalgae proliferation can change benthic communities (Ouisse, Riera, Migné, Leroux, & Davoult, 2011) and increase the community respiration and production (Migné, Ouisse, Hubas, & Davoult, 2011). Benthic microalgae, also called microphytobenthos, excrete extracellular polymeric substances and form a biofilm that can protect the sediment from erosion, storm damage and wave action (Consalvey, Paterson, & Underwood, 2004). They can regulate nutrient fluxes on the sediment–water interface because of the high rate of primary production and by intercepting nutrient outfluxes from sediment. Some tidal flats are highly productive (McIntyre, Geider, & Miller, 1996) and can provide up to two-thirds of the total primary production in estuarine ecosystems (Asmus, 1982). These areas can provide a large amount of primary production (Asmus, 1982; Underwood & Kromkamp, 1999) not only to the benthic food web but also to the planktonic food web by resuspension (De Jonge & Van Beuselom, 1992). Tidal flats can subsidize secondary production in nearby coastal ecosystems through tidal benthic microalgae outwelling (Yoshino et al., 2012), which is also called being a 'carbon donor' (Hill et al., 2015).

The microalgal production on tidal flats was generally higher in the tropical/subtropical region than in the temperate region. Prior studies using the benthic closed-chamber method showed that tidal flats during emersion are small carbon sources (CO_2 outflux) or sinks (CO_2 influx) in temperate regions (Migné, Spilmont, & Davoult, 2004; Spilmont, Davoult, & Migné, 2006). However, using the same method, subtropical tidal flats during emersion showed carbon sinks (Lee, Hsieh, & Lin, 2011). This difference in the net primary production (NPP) of tidal flats was argued to be due to the difference in air temperature (Migné et al., 2009) as ecological processes are generally sensitive to temperature change (Bruno, Carr, & O'Connor, 2015). Seasonal temperature variation has been shown to regulate the production of tidal flats (Hancke & Glud, 2004; Hubas, Davoult, Cariou, & Artigas, 2006; Lee et al., 2011; Migné et al., 2004). Benthic production during emersion would increase 1.2–3.2 times on temperate tidal flats (Hancke & Glud, 2004; Hubas et al., 2006; Migné et al., 2004) and 3.7 times on subtropical tidal flats (Lee et al., 2011) when the air temperature increased by 10°C (i.e. temperature coefficients or Q_{10}). However, the spatial and temporal variability of benthic metabolism on tidal flats along a latitudinal gradient is still unknown. In this study, we determined the primary production and respiration of unvegetated tidal flats along a latitudinal gradient in East Asia; this study included seven sampling sites that ranged approximately 20° in latitude. It was hypothesized that the primary production and respiration on tidal flats would increase along the latitudinal gradient with rising temperature.

2 | MATERIALS AND METHODS

2.1 | Sampling sites and time

To establish a latitudinal gradient, we chose seven tidal flats on the coasts of Taiwan and mainland China ranging from 22.48°N to 40.60°N as our sampling sites (Figure 1; Table 1). This latitudinal gradient extended across approximately 20° in latitude, from tropical to temperate regions.

Measurements at each site were conducted in summer and winter separately from 2012 to 2016. All the measurements were not necessarily conducted in the same year due to manpower and financial constraints. The measurements at CM and DY were conducted in 2012. The measurements at KM and NG were conducted in 2013 and 2014 respectively. The measurements at SY and YK were conducted in 2015. The measurements at GP were conducted from August 2014 to February 2016.

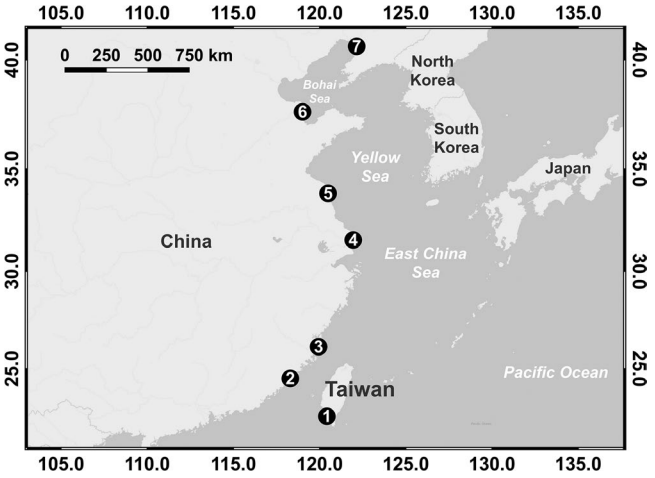

FIGURE 1 Sampling sites for determining the benthic metabolism on tidal flats along a latitudinal gradient in East Asia. The location numbers and names are listed in Table 1

TABLE 1 Locations, studied years and the meteorological conditions of the seven tidal flats along a latitudinal gradient in East Asia

Site		Latitude, longitude	Studied years	Air temperature (°C)		Annual precipitation (mm)
				Minimum	Maximum	
1	Gaoping (GP)	22.48°N, 120.42°E	2014–2016	18.9	29.7	1,589.0[a]
2	Kinmen (KM)	24.49°N, 118.30°E	2013	13.4	27.9	1,400.8
3	Nangan (NG)	26.15°N, 119.94°E	2014	10.0	28.5	908.2
4	Chongming (CM)	31.56°N, 121.95°E	2012	4.4	29.7	1,103.7
5	Sheyang (SY)	33.83°N, 120.49°E	2015	2.7	25.9	1,199.6
6	Dongying (DY)	37.66°N, 119.01°E	2012	−1.8	27.4	515.0
7	Yingkou (YK)	40.60°N, 122.15°E	2015	−6.1	19.9	608.5

[a]The mean of 3 years from 2014 to 2016. https://e-service.cwb.gov.tw/HistoryDataQuery and https://data.cma.cn.

2.2 | Environmental and biological variables

After each field measurement, the sediment characteristics of each sampling site were determined in summer and winter. Sediment samples in the top 5 cm were collected in each chamber by a plastic tube with a diameter of 2.6 cm and taken back to the laboratory for the following measurements. For granulometric analysis, the grain size and silt/clay content of sediments were determined following the standard wet-sieved method (Bale & Kenny, 2005) and the modified pipette method (Hsieh & Chang, 1991) respectively. The content of organic matter in sediments was measured by the loss-on-ignition method (Bale & Kenny, 2005). The sediments were dried at 60°C to a constant weight and then combusted at 500°C for 4 hr; then, the percentage of weight loss was calculated. Sediment interstitial water was collected, stored at 4°C, and taken to the laboratory for nutrient analysis. A spectrophotometer (U-2001; Hitachi) was used for analysing the concentrations of nitrite (Bendschneider & Robinson, 1952), nitrate (Jenkins & Medsker, 1964), ammonia (Pai, Tsau, & Yang, 2001) and phosphate (Murphy & Riley, 1962).

After measuring benthic metabolism, the biomasses of benthic microalgae and macrofauna within benthic chambers were also determined. For collecting benthic microalgae, plastic cores (inner diameter of 1 cm, six replicates in each chamber) were pushed into the sediments to a depth of 1 cm where benthic microalgae are located (Cadée & Hegeman, 1974), and then the sediment samples were frozen until being taken to the laboratory. The chlorophyll *a* concentration was used as an index of the biomass of benthic microalgae, which was determined with the acetone method (Jeffrey & Humphrey, 1975). For collecting macrofauna, stainless steel ring corers with a diameter of 10 cm were pushed into the sediments to a depth of 10 cm. The samples were sieved with a 0.5 mm sieve and taken to the laboratory for sorting, classification, counting and weighing. The macrofauna were dried at 60°C to a constant weight and then combusted at 500°C for 4 hr; the biomass was expressed as the ash-free dry weight per unit surface area.

Meteorological data of the studied year including maximum and minimum air temperature and annual precipitation were derived from the local weather station at each sampling site. The meteorological data at GP, KM and MZ were obtained from the Observation Data Inquire System of Central Weather Bureau, Taiwan (https://e-service.cwb.gov.tw/HistoryDataQuery). The meteorological data at CM, SY, DY and YK were obtained from China Meteorological Data Service Center (https://data.cma.cn).

2.3 | Benthic metabolism measurements

Benthic metabolism on tidal flats in terms of CO_2 fluxes was measured during emersion along the latitudinal gradient by the benthic closed-chamber method which was originally published by Migné et al. (2002) and modified by Lee et al. (2011). The chambers were composed of a semicircular transparent acrylic dome on the top and a stainless steel ring at the bottom. The steel ring, which was 30 cm in diameter and 16 cm in height, was pushed into the sediment to a depth of 10 cm, making an airtight chamber. The gas leak was tested and excluded prior to the measurements. The chamber enclosed a 0.071 m^2 surface area and trapped 10.6 L of air. CO_2 concentration (ppm) exchanges between the sediment and the atmosphere were monitored by an infrared CO_2 gas analyzer (LI-820; LI-COR) for 10 min before the air pressure, temperature and humidity inside chamber obviously elevated. CO_2 concentrations were recorded by a data logger (LI-1400; LI-COR) with a 30 s logging frequency and then regressed against time. The slope of the partial pressure CO_2 (ppm) against time (min) was used to express the change rate in carbon units (mg C m^{-2} hr^{-1}); a molar volume of 24.5 L/mol at normal temperature and pressure and a molar mass of 12 g C/mol CO_2 were assumed. Photosynthetically active radiation (PAR, 400–700 nm, in μmol photons m^{-2} s^{-1}) was measured simultaneously outside the chamber with a quantum sensor (LI-190SA; LI-COR). Sediment temperatures were measured outside the chambers by a temperature sensor (LI-1400–101; LI-COR) and recorded with the same data logger described above.

Benthic metabolism on tidal flats was measured in situ on sunny days under ambient light conditions at noon (10:00–14:00), when the irradiance level was at the saturation level for photosynthesis. Taking tidal effects into consideration, we selected emersions during spring tides. Measurements were taken under ambient light to estimate NPP and in the dark by covering the dome with a piece of opaque curtain to estimate TR. GPP represents the total CO_2 absorption of tidal flat,

which was calculated as the sum of NPP and TR (GPP = NPP + TR). Whenever the sum of NPP and TR was negative, the tidal flat was heterotrophic, and the GPP was assumed to be zero. At each site for each measurement, chambers were exposed in situ in series of five different irradiances of 0%, 30%, 50%, 70% and 100% of shading. This was done by covering screens with different meshes on chambers for measurements of photosynthesis as a function of incident irradiance on the sediment. This function, called P–I curve, was described by the following equation of Jassby and Platt (1976):

$$\mathrm{GPP} = \mathrm{GPP_m} \tanh\left(\frac{\alpha E}{\mathrm{GPP_m}}\right),$$

where GPP_m refers to the maximum GPP (mg C m^{-2} hr^{-1}) in the absence of photoinhibition under optimal irradiance, α is the initial slope of the line under low irradiance when photosynthesis is assumed to be proportional to photon density and E is the irradiance measured as PAR in µmol photons m^{-2} s^{-1}. P–I curves were done by Sigmaplot (version 12.5; Systat Software Inc.) for non-linear regression fitting and results were acceptable when the fit was significant ($p < .05$) and the power of the performed test was >0.80.

We measured CO_2 fluxes of at least 15 randomly chosen (nonrepeating) replicates at each site in each season. Measurements that fell outside the interquartile range (IQR) were considered outliers and were excluded (i.e., between Q1 − 1.5 × IQR and Q3 + 1.5 × IQR, where Q1 is the first quartile, Q3 is the third quartile and IQR is the difference between Q1 and Q3). Although tidal flats were conditioned by the fortnightly periodic tidal inundation (Serôdio & Catarino, 1999), we assumed that the maximum daily NPP of tidal flats occurred when emersion period was during the daytime. Thus, daily GPP_m (g C m^{-2} day^{-1}) was estimated by the sum of GPP_m along the daytime occurring 12 hr in summer and 10 hr in winter. It was also assumed that night-time respiration rates are equal to daytime rates, so that TR (g C m^{-2} hr^{-1}) was extrapolated to estimate 24 hr daily TR (g C m^{-2} day^{-1}). Maximum daily NPP of tidal flats was then calculated as the difference between daily GPP_m and daily TR.

2.4 | Data analysis

The Kruskal–Wallis test was used to examine if the characteristics of the sediment differed among the seven tidal flats because the assumptions of one-way ANOVA were not met for some variables. If significant differences ($p < .05$) were detected, Dunn's multiple comparison test was used to determine which means differed. We conducted the analyses described above in R 3.5.1 (R Core Team, 2018).

3 | RESULTS

During the study years, the maximum air temperature at each site varying between 25.9 and 29.7°C was similar across the latitudinal gradient except the slightly lower value (19.9°C) at YK (Table 1). Minimum air temperature, however, decreased along the latitudinal gradient from the lower-latitude site GP (18.9°C) to the higher-latitude site YK (−6.1°C). Annual precipitation ranging from 515 to 1,589 mm also showed a decreasing trend towards higher latitudes.

All the values of maximum gross primary production (GPP_m), total respiration (TR) and NPP on unvegetated tidal flats during emersion decreased by 100%, 89% and 104% respectively towards higher latitudes in winter, each following an exponential curve (Figure 2a–c). In summer, however, the decreasing trends of GPP_m, TR and NPP towards higher latitudes were not as clear as the latitudinal gradient in winter (Figure 2d–f). The highest value of GPP_m along the latitudinal gradient in winter (GP: 89.68 ± 41.73 mg C m^{-2} hr^{-1}) was comparable to that in summer (GP: 82.64 ± 32.77 mg C m^{-2} hr^{-1}). However, the TR values in summer at each site (3.85 ± 1.41–17.52 ± 14.22 mg C m^{-2} hr^{-1}) were generally higher than in winter (0.80 ± 0.14–15.26 ± 7.50 mg C m^{-2} hr^{-1}). The latitudinal pattern of the NPP on tidal flats was similar to the pattern of the GPP_m with decreasing values towards higher latitudes. The highest value of NPP in winter (GP: 68.07 ± 36.97 mg C m^{-2} hr^{-1}) was also comparable to that in summer (GP: 59.14 ± 26.20 mg C m^{-2} hr^{-1}). It is noted that the values of NPP on tidal flats during emersion at higher latitudes shifted to negative values and became carbon sources in winter.

Our results further found that sediment temperature was effective in predicting the latitudinal variation of benthic metabolism on tidal flats in winter, but not in summer. In winter, the mean sediment temperature decreased along the latitudinal gradient from the lower-latitude site GP (27.6 ± 3.2°C) to the higher-latitude site DY (−1.4 ± 1.8°C; Figure 3). In summer, however, the mean sediment temperature at each site varied between 24.1 and 40.4°C across the latitudinal gradient and no clear pattern could be detected (Figure 3). The higher sediment temperature at KM in summer is likely due to the wide tidal flats and more exposure time to air and irradiance for up to 6 hr at low tide. Benthic metabolism was highly correlated with sediment temperature according to the results of non-linear regression models (Figure 4a–c). The GPP_m was significantly correlated with sediment temperature, which was indicated by a quadratic curve ($y = -0.065x^2 + 3.725x + 0.973$, $r^2 = .175$, $p < .001$). The GPP_m increased as the sediment temperature increased; however, the GPP_m decreased when the sediment temperature was greater than 28.7°C (Figure 4a). The TR was also significantly correlated with sediment temperature via a quadratic relationship ($y = -0.005x^2 + 0.495x - 0.210$, $r^2 = .248$, $p < .001$). TR increased almost linearly from 0 to 45°C and decreased when the sediment temperature was greater than 49.5°C (Figure 4b). The NPP curve was similar to the GPP_m curve, but NPP values started to decrease at lower temperatures when the sediment temperature was greater than 26.6°C (Figure 4c).

4 | DISCUSSION

4.1 | Benthic metabolism along the latitudinal gradient

Despite the spatial variation in sediment features, there was a clear latitudinal gradient of benthic metabolism on tidal flats during

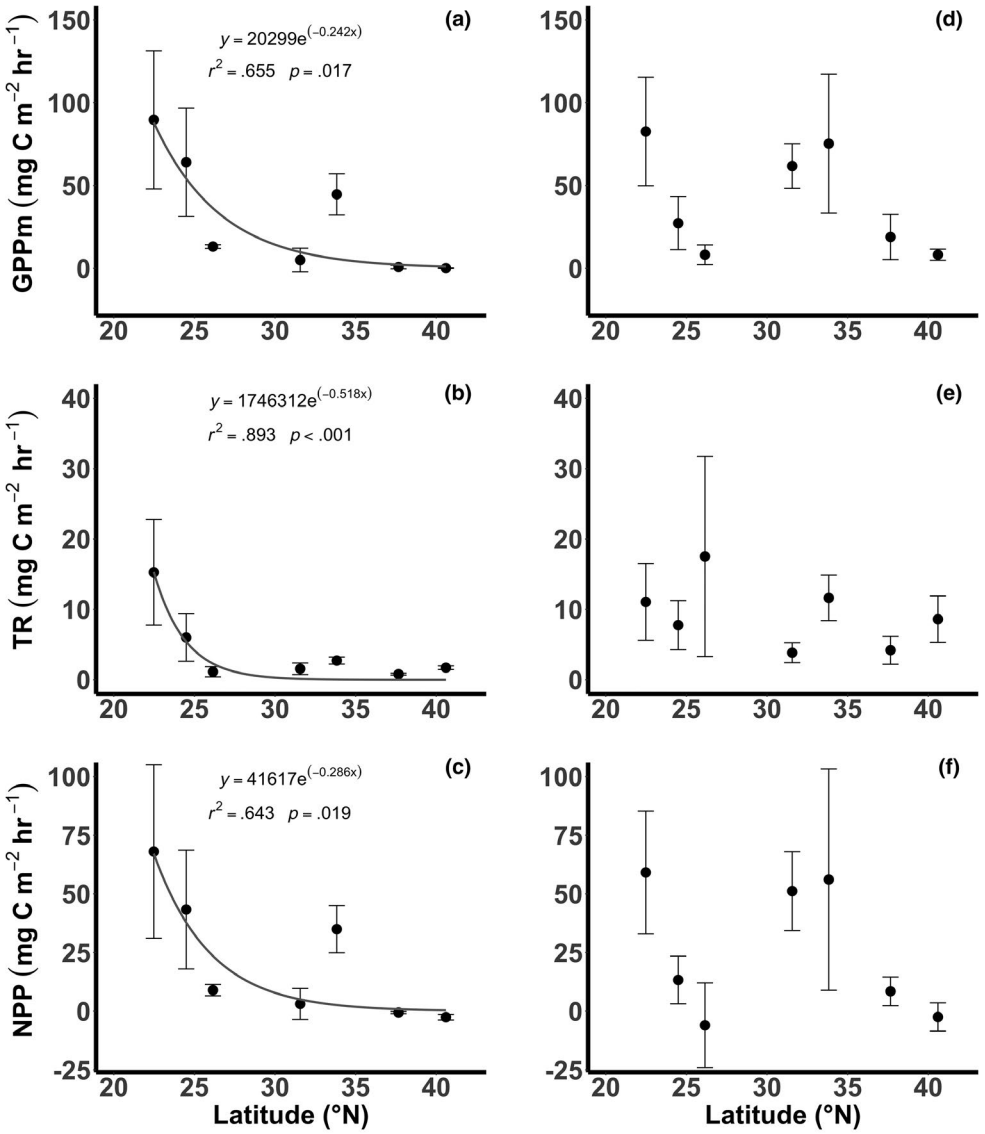

FIGURE 2 Latitudinal gradients of benthic metabolism (GPP_m = maximum gross primary production, TR = total respiration, and NPP = net primary production) on the seven tidal flats in winter (a–c) and summer (d–f). Data are presented as mean ± *SD*

emersion, but the latitudinal gradient varied with season. The clear latitudinal gradient in GPP_m, TR and NPP decreasing exponentially from lower- to higher-latitude from 22.48°N to 40.60°N was observed in winter, but not in summer.

In this study, however, the pattern of benthic production during emersion along the latitudinal gradient was inconsistent with some prior studies using complied data. For example, Lu et al. (2016) compiled CO_2 flux data from 21 coastal wetlands (21.57–52.14°N) and 22 inland wetlands (33.93–72.37°N) worldwide and found that only inland wetlands exhibited decreasing patterns of GPP and NPP with increasing latitude. The authors attributed the reasons to the data that inland wetlands encompass a wider range than coastal wetlands, and the mean annual precipitation showed a significant latitudinal gradient for the inland wetlands but not for the coastal wetlands (Lu et al., 2016). In this study, however, annual precipitation for the tidal flats showed a decreasing trend towards higher latitudes. Coastal vegetation type might greatly affect carbon fluxes (Neff & Hooper, 2002). The 21 coastal wetlands compiled by Lu et al. (2016) included 10 woody and 11 herbaceous ecosystems. The confounding effect of vegetation type could be one major factor for the coastal wetlands in that study exhibiting no latitudinal gradient pattern. For reeds (*Phragmites australis*) growing in tidal wetlands, the net ecosystem exchange (NEE) was estimated to be 376.12 g C m^{-2} $year^{-1}$ in Guandu National Park (25.11°N; Lee, Fan, Wu, & Juang, 2015), which was approximately 5.8 times higher than the NEE also measured for reeds at Panjin Wetland Ecosystem Research Station (41.13°N; Zhou, Zhou, & Jia, 2009). Kirwan, Guntenspergen, and Morris (2009) compiled 56 measurements of salt marsh cordgrass (*S. alterniflora*) productivity on the east coasts of North America and reported a significant decreasing latitudinal gradient across the range from 25.83°N to 45.10°N. However, for eelgrass (*Zostera marina*), annual leaf production revealed no significant regression with temperature from 29.9°N to 56.4°N (Mowll et al., 2015).

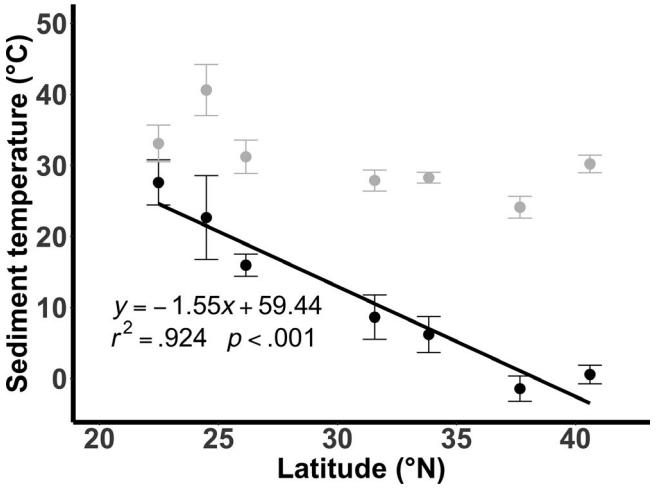

FIGURE 3 Latitudinal gradients of sediment temperature on the seven tidal flats. The solid points represent the measurements taken in winter, and the grey points represent the measurements taken in summer. Data are presented as mean ± *SD*

We did find a clear latitudinal gradient by compiling the results from previous studies that applied different methods to determine the primary production on tidal flats during emersion on the coast of China (Hao et al., 2011; Ning, Liu, & Cai, 1999; Shang, Guan, & Zhang, 2009; Yin et al., 2006). Although the gradients in these studies encompassed a relatively narrow range of latitudes (approximately 10°), both strong relationships between primary production and latitude in winter ($y = -5.613x + 212.769$, $r^2 = .586$, $p = .027$) and in summer ($y = -11.979x + 473.958$, $r^2 = .356$, $p = .040$) existed. Their results in part confirmed our findings in the benthic metabolism on tidal flats during emersion along the wider range of latitudinal gradients.

4.2 | Relationship between benthic metabolism and temperature

Prior studies identified temperature as the main driver for the locally temporal and latitudinal variation of benthic metabolism on tidal flats (Hubas et al., 2006; Lu et al., 2016). Generally, increasing temperature leads to higher metabolic activity levels and photosynthetic rates. The monthly NPP on a subtropical tidal flat during emersion showed a clear seasonal pattern (Lee et al., 2011), and the values were higher in summer and lower in winter, which is in agreement with the findings of the seasonal variation in this study at the tropical and subtropical sites. However, higher temperatures may also increase photoinhibition of epipelic microphytobenthos (Laviale et al., 2015). In this study, the quadratic relationships between benthic metabolism and sediment temperature along the latitudinal gradient were different from the exponential relationships of previous regional studies (Hancke & Glud, 2004; Hubas et al., 2006; Lee et al., 2011; Migné et al., 2004), in which the production and respiration on tidal flats increased with increasing temperature in temperate or subtropical regions. Some other studies reported that the production of benthic microalgae increased progressively with increasing

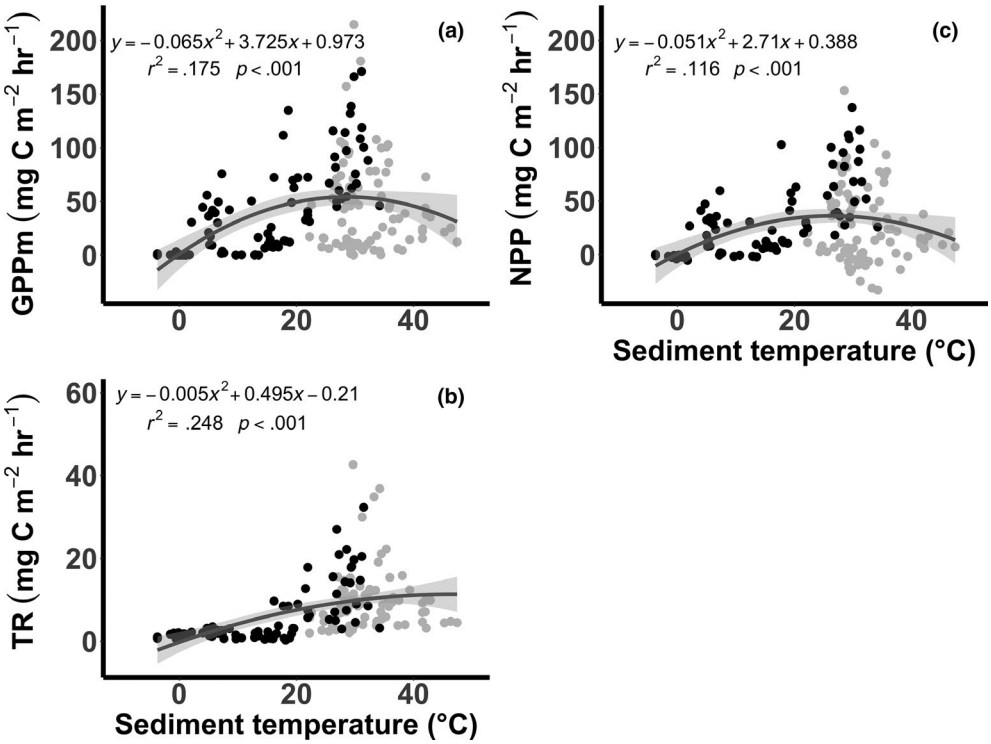

FIGURE 4 Relationships between benthic metabolism (a: GPP_m = maximum gross primary production, b: TR = total respiration, and c: NPP = net primary production) and sediment temperature. The solid points represent the measurements taken in winter, and the grey points represent the measurements taken in summer. Shaded areas around the regression lines indicate 95% confidence intervals

temperature up to an optimum value; beyond that value, the production decreased remarkably. For example, Blanchard, Guarini, Gros, and Richard (1997) measured the response of benthic diatoms in the temperate Bay of Marennes-Oléron (France) to short-term temperature changes in four seasons and estimated that the optimal temperature remained close to 25°C throughout the year. The photosynthetic capacities of two intertidal microphytobenthic communities in the Tagus Estuary (Portugal) increased until the temperature reached 35°C (Vieira, Ribeiro, Marques da Silva, & Cartaxana, 2013). Even on the hypersaline tropical coast of Solar Lake (Egypt), microbial mats composed mainly of diatoms and cyanobacteria had an optimal temperature at 40°C. For the photosynthetic rate of a specific benthic diatom, the optimal temperature values for cultivated *Cylindrotheca closterium* taken from the Ems-Dollard Estuary (the Netherlands) and *Amphora coffeaeformis* obtained from a laboratory culture were 30°C (Morris & Kromkamp, 2003) and 20°C (Salleh & McMinn, 2011) respectively. Our results, which were derived from quadratic models, showed that the GPP_m and NPP reached a maximum value when sediment temperature was nearly 30°C, which is consistent with previous studies. When sediment temperature exceeded this value, the production declined, which is likely due to the impacts of heat stress on the metabolism of benthic microalgae. It has been reported that both photosynthetic activity and the viability of the microalga *Dunaliella salina* decreased significantly due to algal death caused by the degradation of key enzymes and membrane denaturation when the temperature was above 43°C (Béchet, Laviale, Arsapin, Bonnefond, & Bernard, 2017). The production of some benthic microalgae was unable to be detected when the temperature was close to 40°C (Blanchard et al., 1997; Morris & Kromkamp, 2003).

Respiration is also an important temperature-dependent process that has been reported to increase exponentially with temperature. Benthic respiration increased 2.1–5.7 times on temperate tidal flats (Hancke & Glud, 2004; Hubas et al., 2006; Hubas, Lamy, Artigas, & Davoult, 2007) and 4.8 times on a subtropical tidal flat (Lee et al., 2011) in response to a 10°C increase in temperature. Our results also showed that TR increased almost linearly from 0 to 45°C and reached a maximum value when the sediment temperature was 49.5°C (Figure 4c). TR mainly includes autotrophic and heterotrophic respiration. Currently, manipulation studies on how the respiration of benthic microalgae changes with increasing temperature are still lacking. The respiration of diatoms and cyanobacteria on the hypersaline tropical coast of Solar Lake (Egypt) also showed a steady increase in response to elevated temperatures from 15°C to 45°C (Wieland & Kühl, 2000). Bacterial communities generally play a major role in benthic respiration. The contribution of bacteria to benthic respiration was much greater than the contributions of macrofauna and meiofauna (Hubas et al., 2006). In the case of Wimereux sediment on the western coast of France (Hubas et al., 2007), bacterial respiration contributed an average of 80% to the annual benthic respiration. On coastal sediments, the optimal temperatures for oxygen consumption by thermophilic and non-thermophilic bacterial populations were 55 and 30–35°C respectively (Thamdrup, Hansen, & Jørgensen, 1998). Although the bacterial compositions on tidal flats had not yet been examined, our optimal temperature (49.5°C) for the maximum TR derived from this study was consistent with the results of prior studies.

It is noted that the GPP_m and NPP values at SY (33.83°N) deviated a lot from where they should be on the curves (Figure 2). Compared to the nearby lower-latitude sites NG (26.15°N) and CM (31.56°N) along the latitudinal gradient, the significantly higher sediment silt/clay and organic content and the smaller grain size were observed on the tidal flats at SY (Table 2), suggesting that sediment features, particularly organic content and granulometry, can regulate the benthic production on tidal flats during emersion at a local scale (Lee et al., 2011).

4.3 | Assessment of carbon sequestration capacity under land cover change scenarios

During emersion, tidal flats have been reported to be weak carbon sinks or even carbon sources in previous studies (Table 3). However, during immersion periods, increased water turbidity reduced photosynthesis by benthic microalgae (Migné et al., 2009); therefore, tidal flats might act as carbon sources due to the relatively higher respiration rate during the immersion period (Lee et al., 2011). Since benthic microalgae are generally the only primary producers on tidal flats, the NPP on tidal flats can be used to estimate the shift in carbon sequestration capacity under the scenario of degraded vegetated habitats after removal of vascular plants from intertidal zones. The estimate derived from the average across the latitudinal gradient in this study might be able to approach the global mean because large concentrations of tidal flats occur primarily in East Asia with low-sloping coastlines, large tidal ranges and high sediment inflows (Murray et al., 2019). Although the NPP values at latitudes >40°N and <20°N were not included for estimation, the lower values at latitudes >40°N and the higher values at latitudes <20°N according to the latitudinal curve in this study might possibly offset each other. For comparison with vegetated coastal habitats, the hourly NPP in this study was extrapolating to daily NPP. We assumed that daily NPP on tidal flats would reach a maximum value when the emersion period was during daytime, although tidal flats were generally conditioned by the fortnightly periodic tidal inundation. The estimated maximum daily NPP on the tidal flats across the latitudinal gradient averaged 0.236 ± 0.285 g C m^{-2} day^{-1}, which was only 10%–20% of the global average of daily NPP of vegetated coastal habitats (Table 3). Although the global area of unvegetated tidal flats is higher or comparable to that of salt marshes and mangroves (Davidson & Finlayson, 2019), our results suggest that the maximum contribution of NPP on unvegetated tidal flats to the coastal carbon budget is relatively small (11.04 ± 13.32 Tg C/year).

Land cover change influenced by human activities can affect the carbon fluxes and storage ability of the natural landscape (Leite, Costa, Soares-Filho, Hissa, & L., 2012). Vegetated seascapes have been frequently reported to convert to unvegetated

TABLE 2 Sediment features and macrofaunal biomass of the seven tidal flats along a latitudinal gradient in East Asia. Data are presented as the range and mean ± *SD*

Site		Sediment temperature (°C)		Sediment salinity	Sediment organic content (%)	Grain size (μm)	Silt/clay content (%)	Sediment chl*a* concentration (mg/m^2)	Macrofaunal AFDW ($g\ AFDW/m^2$)	Interstitial DIN concentration (μM)	Interstitial DIP concentration (μM)
		winter	summer								
1	Gaoping (GP; *n* = 39)	21.9–31.5 27.6 ± 3.2ab	27.6–35.9 33.1 ± 2.6abc	2.1–29.9 13.7 ± 7.1a	0.8–2.3 1.5 ± 0.3a	10.2–339.2 59.0 ± 68.6 (silt)a	2.7–99.9 73.5 ± 27.0a	1.0–244.0 70.7 ± 58.8ac	0–0.62 0.08 ± 0.14a	2.0–3,942.4 522.8 ± 978.5ab	0.0–3.6 0.8 ± 0.7ab
2	Kinmen (KM; *n* = 34)	17.7–34.2 24.1 ± 5.9ab	34.7–47.4 40.4 ± 3.6d	30.0–35.3 32.6 ± 1.8bc	0.5–3.2 1.6 ± 0.6a	55.3–395.9 166.7 ± 99.4 (fine sand)b	16.6–57.2 29.4 ± 12.0b	77.2–385.6 146.8 ± 66.4bd	0–4.49 0.86 ± 1.23b	11.1–157.4 49.7 ± 37.6ab	0.3–10.4 3.6 ± 2.8ac
3	Nangan (NG; *n* = 24)	13.4–18.8 16.0 ± 1.6b	27.8–34.4 31.2 ± 2.3bc	12.5–41.4 30.0 ± 5.1b	0.6–3.4 1.4 ± 0.7a	126.2–567.8 258.7 ± 96.9 (medium sand)b	0.6–27.9 9.7 ± 8.1b	35.9–219.3 107.9 ± 43.1bd	0–7.64 1.41 ± 2.06b	171–21,915 4,789.6 ± 6,084.1bc	0.5–36.5 5.3 ± 9.4c
4	Chongming (CM; *n* = 23)	5.0–13.5 8.6 ± 3.1bc	26.2–30.0 28.1 ± 1.5bce	0.2–18.0 4.5 ± 5.6d	0.4–4.6 1.7 ± 1.4a	12.3–83.4 42.8 ± 23.9 (silt)a	6.0–98.0 63.5 ± 33.3ab	14.5–169.9 61.4 ± 45.0ac	0–0.83 0.06 ± 0.18a	4.2–492.8 121.2 ± 146.3ab	0.8–9.7 2.3 ± 2.2abc
5	Sheyang (SY; *n* = 22)	2.1 12.3 6.2 ± 2.5bc	27.1–29.5 28.3 ± 0.8bce	5.7–8.8 7.0 ± 0.7ad	2.2–5.8 3.7 ± 1.2b	10.7–28.6 16.2 ± 4.6 (silt)c	92.8–99.9 97.9 ± 2.2c	33.2–149.1 94.1 ± 34.1cd	0–4.06 0.86 ± 1.34b	11.9–608.5 217.7 ± 184.1b	0.0–3.5 0.5 ± 1.0b
6	Dongying (DY; *n* = 17)	−3.8–0.2 −1.4 ± 1.8c	22.2–26.8 24.1 ± 1.5e	7.6–10.8 9.2 ± 0.9ad	2.2–3.4 2.9 ± 0.4b	11.8–32.3 15.8 ± 4.7 (silt)c	95.2–99.7 98.7 ± 1.3c	23.5–161.2 60.7 ± 39.9a	0–0.13 0.001 ± 0.003a	7.0–172.6 36.1 ± 51.9a	0.8–2.3 1.3 ± 0.5abc
7	Yingkou (YK; *n* = 24)	−1.6–3.3 0.6 ± 1.3c	28.6–32.1 30.2 ± 1.2c	37.4–45.0 41.0 ± 2.2c	0.9–4.1 2.8 ± 0.8b	21.1–36.9 27.7 ± 5.0 (silt)ac	57.5–76.9 69.1 ± 5.7a	21.3–88.1 51.0 ± 19.2a	0–0.04 0.002 ± 0.007a	64.4–586.5 195.9 ± 155.4ab	0.8–2.8 1.8 ± 0.7abc

Note: For each variable, different letters after data (mean ± *SD*) indicate significant differences among sites.

Abbreviations: AFDW, ash-free dry weight; chl*a*, chlorophyll *a*; DIN, dissolved inorganic nitrogen ($NO_2 + NO_3 + NH_4$); DIP, dissolved inorganic phosphorus (PO_4).

TABLE 3 Comparison of maximum daily net primary production (NPP) on unvegetated tidal flats in this study with daily NPP of other unvegetated and vegetated habitats

Location	NPP (g C m^{-2} day^{-1})	Global area[a] (10^6 km^2)	Global NPP (Tg C/year)	Reference
Seagrass beds		0.788	310–353	
Global	1.92 ± 0.34			Duarte and Chiscano (1999)
Global	1.079–1.230			Duarte (2017)
Furen Lagoon (43°19′N)	0.624 (summer)			Tokoro et al. (2014)
Southern Taiwan (21°57′N)	0.495–3.735			Chiu et al. (2013)
Dongsha Island (20°42′N)	1.375–7.97			Huang et al. (2015)
Mangroves		0.138	54–138	
Global	1.137			Bouillon et al. (2008)
Global	1.079–2.740			Duarte (2017)
Northern Taiwan (25°08′N)	1.260–3.10			Li et al. (2018)
Salt marshes				
Global	1.200–3.014	0.055	24–60	Duarte (2017)
Eastern US	0.229–1.285			Kirwan et al. (2009)
Unvegetated tidal flats		0.128		
The Bay of Somme (50°13′N)	−0.214			Migné et al. (2004)
The Seine Estuary (49°26′N)	0.068			Spilmont et al. (2006)
Kaomei Wetland (24°18′N)	0.078			Lee et al. (2011)
GP in this study (22°48′N)	0.467 (winter); 0.578 (summer)			This study
YK in this study (40°60′N)	−0.049 (winter); −0.133 (summer)			This study
The latitudinal gradient in this study (22°48′N)–(40°60′N)	0.236 ± 0.285		11.04 ± 13.32	This study

[a]Davidson and Finlayson (2019).

TABLE 4 Global annual loss of net primary production (NPP) resulting from land cover changes from vegetated habitats to unvegetated tidal flats

	Global area[a] (10^6 km^2)	Average annual rate of area change (%)	Change of NPP from vegetated habitats to unvegetated tidal flats (g C m^{-2} day^{-1})	Annual loss of NPP (Tg C/year)
Mangroves	0.138	0.215	1.67	0.181
Seagrass beds	0.778	5.000	0.91	12.921

[a]Global areas of mangroves and seagrass beds were derived from Davidson and Finlayson (2019).

tidal flats by sedimentation (Short et al., 2014; Smith et al., 2009), coastal eutrophication (Deegan et al., 2012; Short et al., 2014), herbicide attacks during a war (Van et al., 2015), overexploitation (Van et al., 2015), alteration of water flow (Cissell, Delgado, Sweetman, & Steinberg, 2018) and aquaculture. The loss of vegetated habitats has been reported to accelerate globally (Davidson & Finlayson, 2019). The area loss rate of mangroves and seagrass beds averaged 0.22% per year and 5% per year respectively. Despite no global area change available for salt marshes, the global area of salt marshes is also considered qualitatively declining (Davidson & Finlayson, 2019). If the land cover of these vegetated habitats is changed to unvegetated tidal flats, the carbon sequestration capacity in coastal blue carbon ecosystems would reduce at least by 13.10 Tg C/year if the trend in decline continues (Table 4). The reduction rate in carbon sequestration capacity due to the decline of coastal vegetated habitats is equivalent to 1% of carbon emissions from land-use change (1.3 ± 0.7 Gt C/year; Friedlingstein et al., 2019).

ACKNOWLEDGEMENTS

This study was financially supported by Kinmen National Park Headquarter, Mainland Affairs Council of Taiwan, National Natural Science Foundation of China (grant nos. U1405234 and 41871035) and the 'Innovation and Development Center of Sustainable

Agriculture' from The Featured Areas Research Center Program within the Higher Education Sprout Project by the Ministry of Education (MOE) of Taiwan. We appreciate the help of Chung-Ming Yeh, En-Tse Chang, Mingyao Huang and Qiang Sheng in the field.

CONFLICT OF INTERESTS

The authors declare no competing financial interests.

AUTHORS' CONTRIBUTIONS

W.J.L. and H.J.L. conceived and designed the study, contributed to the data analysis, interpretation and manuscript writing. W.J.L. and J.W. carried out the field work and sampling quantification.

DATA AVAILABILITY STATEMENT

Figures 2 and 3 and Table 2 have associated raw data. We encourage prospective data users to contact us before embarking on any analysis.

ORCID

Wei-Jen Lin https://orcid.org/0000-0002-9217-5267
Hsing-Juh Lin https://orcid.org/0000-0001-8322-7195

REFERENCES

Asmus, R. (1982). Field measurements on several variation of the activity of primary producers on a sandy tidal flat in the northern Wadden Sea. *Netherlands Journal of Sea Research*, *16*, 389–402. https://doi.org/10.1016/0077-7579(82)90045-x

Bale, A. J., & Kenny, A. J. (2005). Sediment analysis and seabed characterisation. In A. Eleftheriou & A. McIntyre (Eds.), *Methods for the study of marine benthos* (3rd ed., pp. 43–86). Oxford, UK: Blackwell Science Ltd.

Béchet, Q., Laviale, M., Arsapin, N., Bonnefond, H., & Bernard, O. (2017). Modeling the impact of high temperatures on microalgal viability and photosynthetic activity. *Biotechnology for Biofuels*, *10*(1), 1–11. https://doi.org/10.1186/s13068-017-0823-z

Bendschneider, K., & Robinson, R. J. (1952). A new spectrophotometric method for the determination of nitrite in sea water. *Journal of Marine Research*, *11*, 87–96.

Blanchard, G. F., Guarini, J. M., Gros, P., & Richard, P. (1997). Seasonal effect on the relationship between the photosynthetic capacity of intertidal microphytobenthos and temperature. *Journal of Phycology*, *33*(5), 723–728. https://doi.org/10.1111/j.0022-3646.1997.00723.x

Bouillon, S., Borges, A. V., Castañeda-Moya, E., Diele, K., Dittmar, T., Duke, N. C., … Twilley, R. R. (2008). Mangrove production and carbon sinks: A revision of global budget estimates. *Global Biogeochemical Cycles*, *22*(2). https://doi.org/10.1029/2007GB003052

Bruno, J. F., Carr, L. A., & O'Connor, M. I. (2015). Exploring the role of temperature in the ocean through metabolic scaling. *Ecology*, *96*(12), 3126–3140. https://doi.org/10.1890/14-1954.1

Cadée, G. C., & Hegeman, J. (1974). Primary production of the benthic microflora living on tidal flats in the Dutch Wadden Sea. *Netherlands Journal of Sea Research*, *8*(2–3), 260–291. https://doi.org/10.1016/0077-7579(74)90020-9

Chen, Y., Dong, J., Xiao, X., Zhang, M., Tian, B. O., Zhou, Y., … Ma, Z. (2016). Land claim and loss of tidal flats in the Yangtze Estuary. *Scientific Reports*, *6*(1), 24018. https://doi.org/10.1038/srep24018

Chiu, S. H., Huang, Y. H., & Lin, H. J. (2013). Carbon budget of leaves of the tropical intertidal seagrass *Thalassia hemprichii*. *Estuarine, Coastal and Shelf Science*, *125*, 27–35. https://doi.org/10.1016/j.ecss.2013.03.026

Cissell, J. R., Delgado, A. M., Sweetman, B. M., & Steinberg, M. K. (2018). Monitoring mangrove forest dynamics in Campeche, Mexico, using Landsat satellite data. *Remote Sensing Applications: Society and Environment*, *9*, 60–68. https://doi.org/10.1016/j.rsase.2017.12.001

Consalvey, M., Paterson, D. M., & Underwood, G. J. C. (2004). The ups and downs of life in a benthic biofilm: Migration of benthic diatoms. *Diatom Research*, *19*(2), 181–202. https://doi.org/10.1080/0269249X.2004.9705870

Costanza, R., d'Arge, R., de Groot, R., Farber, S., Grasso, M., Hannon, B., … van den Belt, M. (1997). The value of the world's ecosystem services and natural capital. *Nature*, *387*(6630), 253–260. https://doi.org/10.1038/387253a0

Davidson, N. C., & Finlayson, C. M. (2019). Updating global coastal wetland areas presented in Davidson and Finlayson (2018). *Marine and Freshwater Research*, *70*(8), 1195–1200. https://doi.org/10.1071/MF19010

De Jonge, V. N., & Van Beuselom, J. E. E. (1992). Contribution of resuspended microphytobenthos to total phytoplankton in the EMS estuary and its possible role for grazers. *Netherlands Journal of Sea Research*, *30*(C), 91–105. https://doi.org/10.1016/0077-7579(92)90049-K

Deegan, L. A., Johnson, D. S., Warren, R. S., Peterson, B. J., Fleeger, J. W., Fagherazzi, S., & Wollheim, W. M. (2012). Coastal eutrophication as a driver of salt marsh loss. *Nature*, *490*(7420), 388–392. https://doi.org/10.1038/nature11533

Duarte, C. M. (2017). Reviews and syntheses: Hidden forests, the role of vegetated coastal habitats in the ocean carbon budget. *Biogeosciences*, *14*(2), 301–310. https://doi.org/10.5194/bg-14-301-2017

Duarte, C. M., & Chiscano, C. L. (1999). Seagrass biomass and production: A reassessment. *Aquatic Botany*, *65*(1–4), 159–174. https://doi.org/10.1016/S0304-3770(99)00038-8

Friedlingstein, P., Jones, M. W., O'Sullivan, M., Andrew, R. M., Hauck, J., Peters, G. P., … Zaehle, S. (2019). Global carbon budget 2019. *Earth System Science Data*, *11*, 1783–1838. https://doi.org/10.3929/ethz-b-000385668

Galbraith, H., Jones, R., Park, R., Clough, J., Herrod-Julius, S., Harrington, B., & Page, G. (2002). Global climate change and sea level rise: Potential losses of intertidal habitat for shorebirds. *Waterbirds*, *25*(2), 173–183. https://doi.org/10.1675/1524-4695(2002)025[0173:gccasl]2.0.co;2

Hancke, K., & Glud, R. N. (2004). Temperature effects on respiration and photosynthesis in three diatom-dominated benthic communities. *Aquatic Microbial Ecology*, *37*(3), 265–281. https://doi.org/10.3354/ame037265

Hao, Q., Cai, Y., Ning, X., Liu, C., Peng, X., & Tang, X. (2011). Standing crop and primary production of benthic microalgae on the tidal flats in Yueqing Bay. *Journal of Ocean University of China*, *10*(2), 157–164. https://doi.org/10.1007/s11802-011-1750-4

Hill, R., Bellgrove, A., Macreadie, P. I., Petrou, K., Beardall, J., Steven, A., & Ralph, P. J. (2015). Can macroalgae contribute to blue carbon? An Australian perspective. *Limnology and Oceanography*, *60*(5), 1689–1706. https://doi.org/10.1002/lno.10128

Hsieh, H. L., & Chang, K. H. (1991). Habitat characteristics and occurrence of the spionid *Pseudopolydora* sp on the tube-caps of the onuphid *Diopatra bilobata* (Polychaeta: *Spionidae Onuphidae*). *Bulletin of the Institute of Zoology Academia Sinica*, *30*(4), 331–339.

Huang, Y. H., Lee, C. L., Chung, C. Y., Hsiao, S. C., & Lin, H. J. (2015). Carbon budgets of multispecies seagrass beds at Dongsha Island in the South China Sea. *Marine Environmental Research*, *106*, 92–102. https://doi.org/10.1016/j.marenvres.2015.03.004

Hubas, C., Davoult, D., Cariou, T., & Artigas, L. F. (2006). Factors controlling benthic metabolism during low tide along a granulometric gradient in an intertidal bay (Roscoff Aber Bay, France). *Marine Ecology Progress Series*, *316*, 53–68. https://doi.org/10.3354/meps316053

Hubas, C., Lamy, D., Artigas, L. F., & Davoult, D. (2007). Seasonal variability of intertidal bacterial metabolism and growth efficiency in an exposed sandy beach during low tide. *Marine Biology*, *151*(1), 41–52. https://doi.org/10.1007/s00227-006-0446-6

Jassby, A. D., & Platt, T. (1976). Mathematical formulation of the relationship between photosynthesis and light for phytoplankton. *Limnology and Oceanography*, *21*(4), 540–547. https://doi.org/10.4319/lo.1976.21.4.0540

Jeffrey, S. W., & Humphrey, G. F. (1975). New spectrophotometric equations for determining chlorophylls *a*, *b*, *c*1 and *c*2 in higher plants, algae and natural phytoplankton. *Biochemie Und Physiologie Der Pflanzen*, *167*(2), 191–194. https://doi.org/10.1016/S0015-3796(17)30778-3

Jenkins, D., & Medsker, L. L. (1964). Brucine method for determination of nitrate in ocean, estuarine, and fresh waters. *Analytical Chemistry*, *36*(3), 610–612. https://doi.org/10.1021/ac60209a016

Kirwan, M. L., Guntenspergen, G. R., & Morris, J. T. (2009). Latitudinal trends in *Spartina alterniflora* productivity and the response of coastal marshes to global change. *Global Change Biology*, *15*(8), 1982–1989. https://doi.org/10.1111/j.1365-2486.2008.01834.x

Kirwan, M. L., & Megonigal, J. P. (2013). Tidal wetland stability in the face of human impacts and sea-level rise. *Nature*, *504*(7478), 53–60. https://doi.org/10.1038/nature12856

Laviale, M., Barnett, A., Ezequiel, J., Lepetit, B., Frankenbach, S., Méléder, V., … Lavaud, J. (2015). Response of intertidal benthic microalgal biofilms to a coupled light-temperature stress: Evidence for latitudinal adaptation along the Atlantic coast of Southern Europe. *Environmental Microbiology*, *17*(10), 3662–3677. https://doi.org/10.1111/1462-2920.12728

Lee, L. H., Hsieh, L. Y., & Lin, H. J. (2011). *In situ* production and respiration of the benthic community during emersion on subtropical intertidal sandflats. *Marine Ecology Progress Series*, *441*, 33–47. https://doi.org/10.3354/meps09362

Lee, S. C., Fan, C. J., Wu, Z. Y., & Juang, J. Y. (2015). Investigating effect of environmental controls on dynamics of CO_2 budget in a subtropical estuarial marsh wetland ecosystem. *Environmental Research Letters*, *10*(2), 25005. https://doi.org/10.1088/1748-9326/10/2/025005

Leite, C. C., Costa, M. H., Soares-Filho, B. S., & De Barros Viana Hissa, L. (2012). Historical land use change and associated carbon emissions in Brazil from 1940 to 1995. *Global Biogeochemical Cycles*, *26*(2), 1–13. https://doi.org/10.1029/2011GB004133

Li, B. O., Liao, C.-H., Zhang, X.-D., Chen, H.-L., Wang, Q., Chen, Z.-Y., … Chen, J.-K. (2009). *Spartina alterniflora* invasions in the Yangtze River estuary, China: An overview of current status and ecosystem effects. *Ecological Engineering*, *35*(4), 511–520. https://doi.org/10.1016/j.ecoleng.2008.05.013

Li, S. B., Chen, P. H., Huang, J. S., Hsueh, M. L., Hsieh, L. Y., Lee, C. L., & Lin, H. J. (2018). Factors regulating carbon sinks in mangrove ecosystems. *Global Change Biology*, *24*(9), 4195–4210. https://doi.org/10.1111/gcb.14322

Lin, H. J., Hsu, C. B., Liao, S. H., Chen, C. P., & Hsieh, H. L. (2015). Effects of *Spartina alterniflora* invasion on the abundance and community of meiofauna in a subtropical wetland. *Wetlands*, *35*, 547–556. https://doi.org/10.1007/s13157-015-0643-5

Lu, W., Xiao, J., Liu, F., Zhang, Y., Liu, C., & Lin, G. (2016). Contrasting ecosystem CO_2 fluxes of inland and coastal wetlands: A meta-analysis of eddy covariance data. *Global Change Biology*, *23*(3), 1180–1198. https://doi.org/10.1111/gcb.13424

McIntyre, H. L., Geider, R. J., & Miller, D. C. (1996). Microphytobenthos: The ecological role of the "Secret Garden" of unvegetated, shallow-water marine habitats. I. Distribution, abundance and primary production. *Estuaries*, *19*, 185–201. https://doi.org/10.2307/1352224

Migné, A., Davoult, D., Spilmont, N., Menu, D., Boucher, G., Gattuso, J. P., & Rybarczyk, H. (2002). A closed-chamber CO_2-flux method for estimating intertidal primary production and respiration under emersed conditions. *Marine Biology*, *140*(4), 865–869. https://doi.org/10.1007/s00227-001-0741-1

Migné, A., Ouisse, V., Hubas, C., & Davoult, D. (2011). Freshwater seepages and ephemeral macroalgae proliferation in an intertidal bay: II. Effect on benthic biomass and metabolism. *Estuarine, Coastal and Shelf Science*, *92*(1), 161–168. https://doi.org/10.1016/j.ecss.2010.12.023

Migné, A., Spilmont, N., Boucher, G., Denis, L., Hubas, C., Janquin, M.-A., … Davoult, D. (2009). Annual budget of benthic production in Mont Saint-Michel Bay considering cloudiness, microphytobenthos migration, and variability of respiration rates with tidal conditions. *Continental Shelf Research*, *29*(19), 2280–2285. https://doi.org/10.1016/j.csr.2009.09.004

Migné, A., Spilmont, N., & Davoult, D. (2004). *In situ* measurements of benthic primary production during emersion: Seasonal variations and annual production in the Bay of Somme (eastern English Channel, France). *Continental Shelf Research*, *24*(13–14), 1437–1449. https://doi.org/10.1016/j.csr.2004.06.002

Morris, E. P., & Kromkamp, J. C. (2003). Influence of temperature on the relationship between oxygen- and fluorescence-based estimates of photosynthetic parameters in a marine benthic diatom (*Cylindrotheca closterium*). *European Journal of Phycology*, *38*, 133–142. https://doi.org/10.1080/0967026031000085832

Mowll, W., Blumenthal, D. M., Cherwin, K., Smith, A., Symstad, A. J., Vermeire, L. T., … Knapp, A. K. (2015). Climatic controls of aboveground net primary production in semi-arid grasslands along a latitudinal gradient portend low sensitivity to warming. *Oecologia*, *177*(4), 959–969. https://doi.org/10.1007/s00442-015-3232-7

Murphy, J., & Riley, J. P. (1962). A modified single solution method for the determination of phosphate in natural waters. *Analytica Chimica Acta*, *27*, 31–36. https://doi.org/10.1057/9781137461131

Murray, N. J., Clemens, R. S., Phinn, S. R., Possingham, H. P., & Fuller, R. A. (2014). Tracking the rapid loss of tidal wetlands in the Yellow Sea. *Frontiers in Ecology and the Environment*, *12*(5), 267–272. https://doi.org/10.1890/130260

Murray, N. J., Phinn, S. R., DeWitt, M., Ferrari, R., Johnston, R., Lyons, M. B., … Fuller, R. A. (2019). The global distribution and trajectory of tidal flats. *Nature*, *565*, 222–225. https://doi.org/10.1038/s41586-018-0805-8

Neff, J. C., & Hooper, D. U. (2002). Vegetation and climate controls on potential CO_2, DOC and DON production in northern latitude soils. *Global Change Biology*, *8*(9), 872–884. https://doi.org/10.1046/j.1365-2486.2002.00517.x

Nellemann, C., Corcoran, E., Duarte, C. M., Valdés, L., De Young, C., Fonseca, L., & Grimsditch, G. (2009). *Blue carbon. A rapid response assessment*. Birkeland, Norway: United Nations Environment Programme, GRID-Arendal, Birkeland Trykkeri AS.

Ning, X., Liu, Z., & Cai, Y. (1999). Standing crop and productivity of the benthic microflora living in tidal flats of the Xiangshan Bay. *Acta Oceanologica Sinica*, *21*(3), 98–105.

Ouisse, V., Riera, P., Migné, A., Leroux, C., & Davoult, D. (2011). Freshwater seepages and ephemeral macroalgae proliferation in an intertidal bay: I. Effect on benthic community structure and food web. *Estuarine, Coastal and Shelf Science*, *91*, 272–281. https://doi.org/10.1016/j.ecss.2010.10.034

Pai, S. C., Tsau, Y. J., & Yang, T. I. (2001). pH and buffering capacity problems involved in the determination of ammonia in saline water using the indophenol blue spectrophotometric method. *Analytica Chimica Acta*, *434*(2), 209–216. https://doi.org/10.1016/S0003-2670(01)00851-0

R Core Team. (2018). *R: A language and environment for statistical computing*. Vienna, Austria: R Foundation for Statistical Computing.

Salleh, S., & McMinn, A. (2011). The effects of temperature on the photosynthetic parameters and recovery of two temperate benthic microalgae, *Amphora* cf. *coffeaeformis* and *Cocconeis* cf. *sublittoralis*

(Bacillariophyceae). *Journal of Phycology*, *47*(6), 1413–1424. https://doi.org/10.1111/j.1529-8817.2011.01079.x

Serôdio, J., & Catarino, F. (1999). Fortnightly light and temperature variability in estuarine intertidal sediments and implications for microphytobenthos primary productivity. *Aquatic Ecology*, *33*, 235–241. https://doi.org/10.1023/a:1009989229098

Shang, X., Guan, W. B., & Zhang, J. (2009). Distribution characteristics and contribution to total primary production of microphytobenthos in the salt marshes of the Changjiang Estuary. *Acta Oceanologica Sinica*, *31*(5), 40–47.

Short, F. T., Coles, R., Fortes, M. D., Victor, S., Salik, M., Isnain, I., … Seno, A. (2014). Monitoring in the Western Pacific region shows evidence of seagrass decline in line with global trends. *Marine Pollution Bulletin*, *83*(2), 408–416. https://doi.org/10.1016/j.marpolbul.2014.03.036

Smith, T. J., Anderson, G. H., Balentine, K., Tiling, G., Ward, G. A., & Whelan, K. R. T. (2009). Cumulative impacts of hurricanes on Florida mangrove ecosystems: Sediment deposition, storm surges and vegetation. *Wetlands*, *29*(1), 24–34. https://doi.org/10.1672/08-40.1

Spilmont, N., Davoult, D., & Migné, A. (2006). Benthic primary production during emersion: In situ measurements and potential primary production in the Seine Estuary (English Channel, France). *Marine Pollution Bulletin*, *53*(1–4), 49–55. https://doi.org/10.1016/j.marpolbul.2005.09.016

Thamdrup, B., Hansen, J. W., & Jørgensen, B. B. (1998). Temperature dependence of aerobic respiration in a coastal sediment. *FEMS Microbiology Ecology*, *25*(2), 189–200. https://doi.org/10.1016/S0168-6496(97)00095-0

Tokoro, T., Hosokawa, S., Miyoshi, E., Tada, K., Watanabe, K., Montani, S., … Kuwae, T. (2014). Net uptake of atmospheric CO_2 by coastal submerged aquatic vegetation. *Global Change Biology*, *20*(6), 1873–1884. https://doi.org/10.1111/gcb.12543

Underwood, G. J. G., & Kromkamp, J. (1999). Primary production by phytoplankton and microphytobenthos in estuaries. *Advances in Ecological Research*, *29*, 93–153. https://doi.org/10.1016/s0065-2504(08)60192-0

Van, T. T., Wilson, N., Thanh-Tung, H., Quisthoudt, K., Quang-Minh, V., Xuan-Tuan, L., … Koedam, N. (2015). Changes in mangrove vegetation area and character in a war and land use change affected region of Vietnam (Mui Ca Mau) over six decades. *Acta Oecologica*, *63*, 71–81. https://doi.org/10.1016/j.actao.2014.11.007

Vieira, S., Ribeiro, L., Marques da Silva, J., & Cartaxana, P. (2013). Effects of short-term changes in sediment temperature on the photosynthesis of two intertidal microphytobenthos communities. *Estuarine, Coastal and Shelf Science*, *119*, 112–118. https://doi.org/10.1016/j.ecss.2013.01.001

Wieland, A., & Kühl, M. (2000). Irradiance and temperature regulation of oxygenic photosynthesis and O_2 consumption in a hypersaline cyanobacterial mat (Solar Lake, Egypt). *Marine Biology*, *137*, 71–85. https://doi.org/10.1007/s002270000331

Yin, H., Sun, Y., Shi, X. Y., Jiang, S. X., Meng, W., Song, J. Z., & Chen, Y. Z. (2006). Biomass and primary productivity of the microphytobenthos on mudflats of the Rushan Bay east flow area. *Marine Fisheries Research*, *27*, 62–66.

Yoshino, K., Tsugeki, N. K., Amano, Y., Hayami, Y., Hamaoka, H., & Omori, K. (2012). Intertidal bare mudflats subsidize subtidal production through outwelling of benthic microalgae. *Estuarine, Coastal and Shelf Science*, *109*, 138–143. https://doi.org/10.1016/j.ecss.2012.05.021

Zhou, L., Zhou, G., & Jia, Q. (2009). Annual cycle of CO_2 exchange over a reed (*Phragmites australis*) wetland in Northeast China. *Aquatic Botany*, *91*, 91–98. https://doi.org/10.1016/j.aquabot.2009.03.002

How to cite this article: Lin W-J, Wu J, Lin H-J. Contribution of unvegetated tidal flats to coastal carbon flux. *Glob Change Biol*. 2020;26:3443–3454. https://doi.org/10.1111/gcb.15107